Electronic Supplementary Material (ESI) for Journal of Materials Chemistry A.

Large-area, Green Solvent Spray Deposited Nickel Oxide Films for Scalable Fabrication of Triple-Cation Perovskite Solar Cells

*Neetesh Kumar[1], Hock Beng Lee[1], Sunbin Hwang[2] and Jae-Wook Kang[1]**

[1]Department of Flexible and Printable Electronics, LANL-CBNU Engineering Institute-Korea, Chonbuk National University, Jeonju 54896, Republic of Korea.

[2]Functional Composite Materials Research Center, Institute of Advanced Composite Materials, Korea Institute of Science and Technology,Wanju-gun 55324, Republic of Korea

*Corresponding author: Prof. Jae-Wook Kang

E-mail: jwkang@jbnu.ac.kr

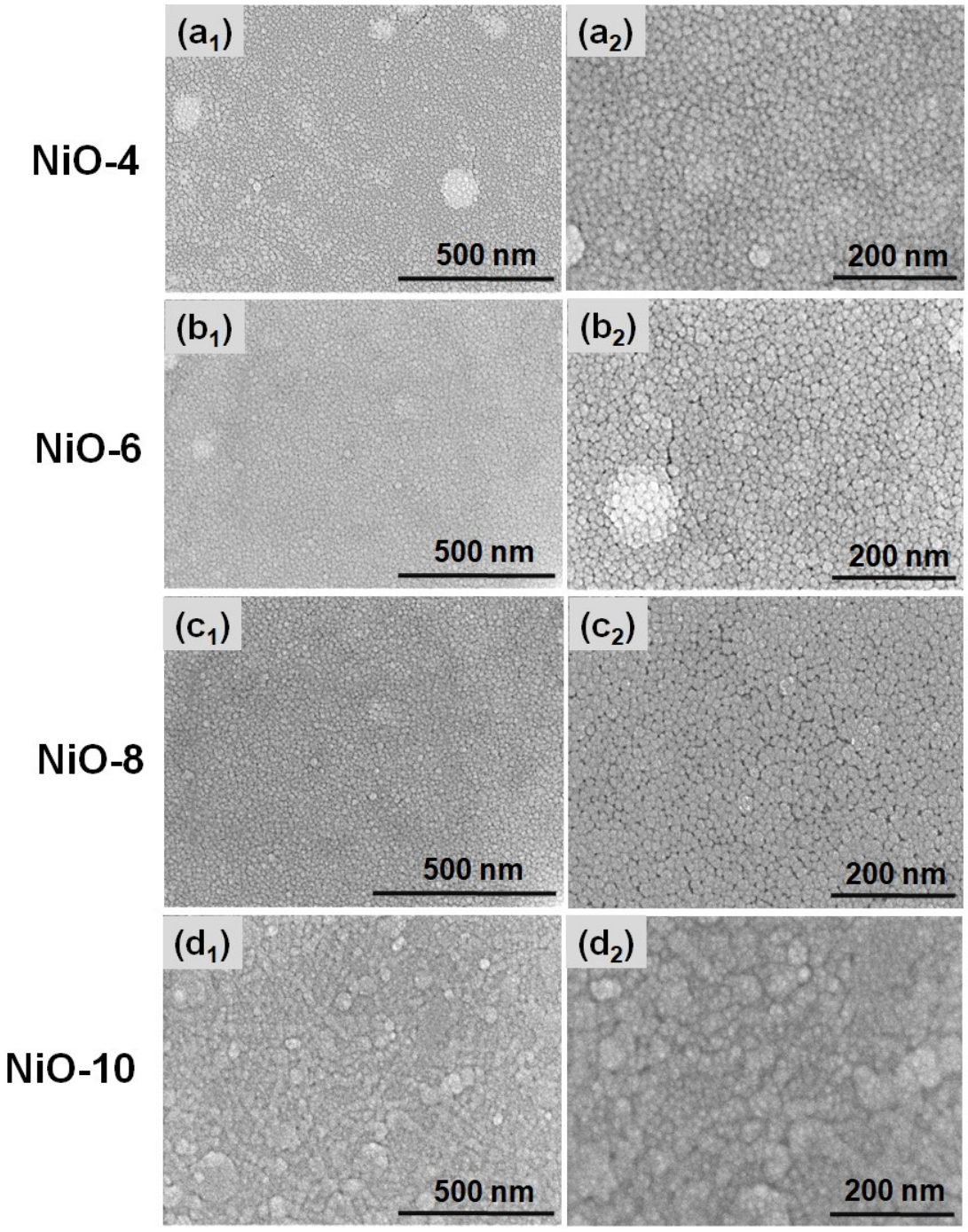

Fig. S1. Low and high magnification FE-SEM images of spray deposited NiO films on ITO substrates showing the change in surface morphology with spray cycles. (a_1, a_2) 4 spray cycles, (b_1, b_2) 6-spray cycles, (c_1, c_2) 8-spray cycles, and (d_1, d_2) 10-spray cycles.

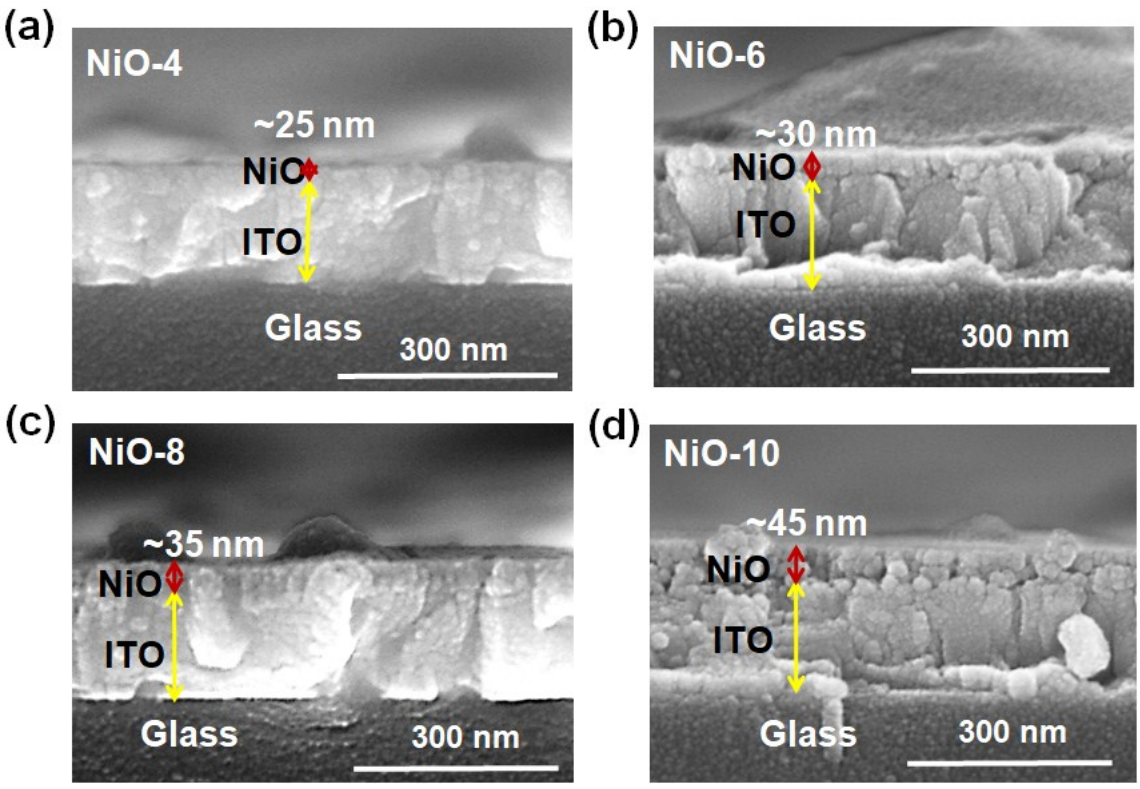

Fig. S2. Cross-sectional FE-SEM images of (a) NiO-4, (b) NiO-6, (c) NiO-8 and (d) NiO-10 films deposited on ITO substrates.

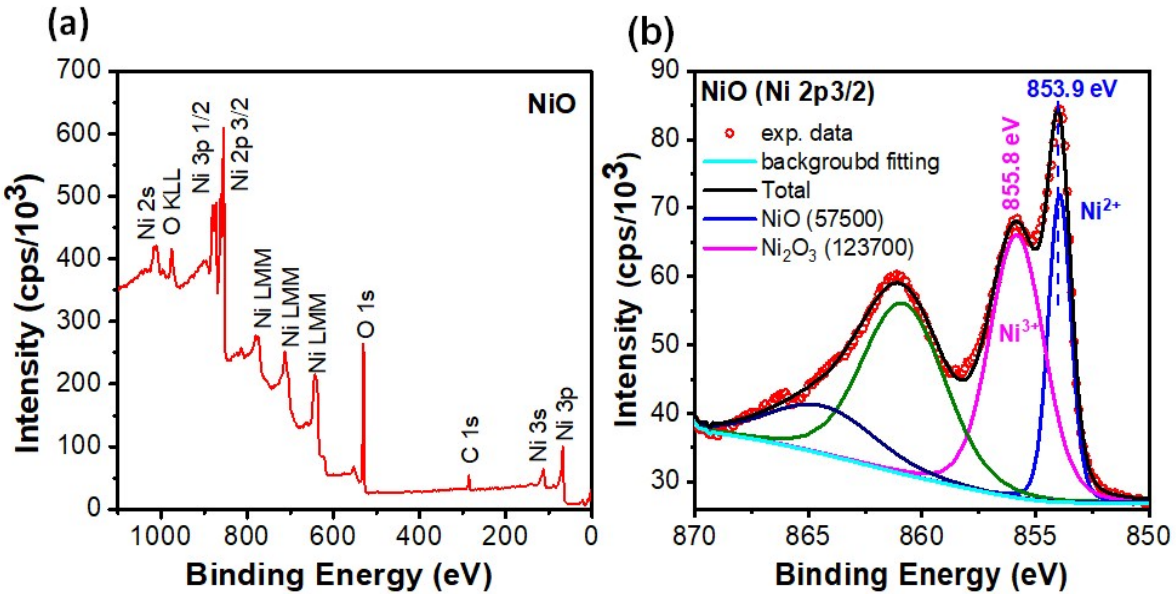

Fig. S3. (a) Representative wide-scan XPS survey spectrum and (b) high resolution scan spectra of the Ni 2p3/2 peak of NiO thin film.

UPS Analysis

The energy levels of NiO were examined via UPS analysis. The energy difference (E_i) between the valence band maximum (E_{VB}) and E_F is derived from the low binding energy tails. The work function, or Fermi level (E_F) of the charge carrier extraction layers are obtained by subtracting the binding energies of the secondary electron cutoffs from the excitation energy (21.22 eV) of He^I UPS spectra. The position of the valence band was confirmed using the equation E_{VB} = 21.22–(E_{cutoff} – E_i). Based on the tails at low binding energy, the energy difference (E_i) between Fermi level (E_F) and the valence band maximum (E_{vb}) is about ~0.36 eV, and the work function or Fermi level was approximately -4.52 eV. This was determined by subtracting the $E_{cut\text{-}off}$ (16.7 eV) from the excitation energy (21.22 eV) of He^I. The position of the valence band (VB) energy level was an energy of -4.88 eV. After determining the E_{VB}, the conduction band (E_{CB}) energy level can be obtained easily by adding the optical bad gap (~3.70 eV) to the E_{VB} (~4.88 eV). Therefore, the E_{CB} of the NiO film was approximately -1.18 eV.

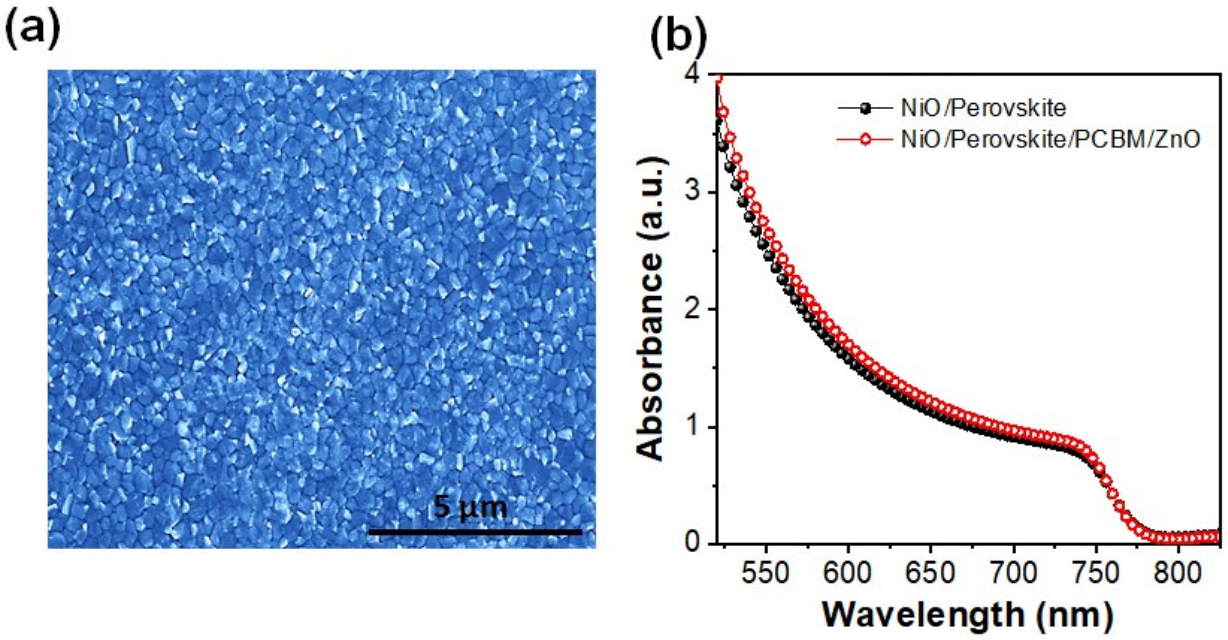

Fig. S4. (a) Low-magnification FESEM images of perovskite films deposited on the top NiO-8 HTL and (b) absorbance spectra with HTL and HTL-ETL layers.

TRPL analysis:

The TRPL decay parameters were obtained by fitting the decay profile data using the bi-exponential function as:

$$Y(t) = A_1 \exp\left(-\frac{t - t_0}{t_1}\right) + A_1\left(-\frac{t - t_0}{t_2}\right) + Y_0 \quad (1)$$

Here, τ_1 and τ_2 are the first and second order decay times, and A_1 and A_2 are the respective weight factors of each decay channel. The fast-decay time (τ_1) indicates the non-radiative decay, and the slow-decay (τ_2) indicates the radiative decay, which originated from the recombination of charge carriers and free-charge carriers before the collection, respectively. The average recombination lifetime $<\tau_{avg}>$ was calculated from the following equation:

$$<\tau_{Avg}> = \frac{A_1\tau_1^2 + A_1\tau_2^2}{A_1\tau_1 + A_2\tau_2} \quad (2)$$

Table S1. TRPL lifetime measurements of perovskite absorber deposited on an ITO/NiOx-8 coated substrate. Weight fraction calculated from the amplitude at a particular lifetime decay.

Sample	**τ_1 (ns)**	**τ_2 (ns)**	**A_1**	**A_2**	**<τ> (ns)**
ITO/pero.	2.058	15.891	0.2138	0.3467	14.85
ITO/NiO/pero.	1.271	10.540	0.2454	0.3113	9.73
ITO/NiO/Pero./PCBM/ZnO	1.232	9.0310	0.3411	0.2684	7.87

Table S2. Summary of device parameters V_{OC}, J_{SC}, FF, and PCE of the inverted PSCs using undoped spray deposited NiO or NiO_x HTLs with device configurations and antisolvents used for depositing the perovskite layer.

HTL	Method (solvent)	Anti-Solvent (vol.)	Perovskite System	V_{oc} (V)	J_{sc} (mA cm^{-1})	FF (%)	PCE (%)	Ref.
NiO	Spray[a]	Toluene (800 µL)	FTO/NiO/$MAPbI_3$/PCBM/TiO_x/Ag	1.03	18.70	64.0	12.4	[1]
NiO	Spray[a]	Toluene (800 µL)	FTO/NiO/$MAPbI_3$/PCBM/BCP/Ag	1.09	20.26	74.8	16.6	[2]
NiO	Spray[a]	Toluene (800 µL)	FTO/NiO-Al_2O_3/$MAPbI_3$/PCBM/BCP/Ag	1.04	18.0	72.0	13.5	[3]
NiO	Spray Combustion[b]	Methylbenzene (1000 µL)	FTO/NiO/$MAPbI_3$/PCBM//Ag	1.03	17.42	71.2	12.7	[4]
NiO	Ultrasonic Spray[c]	N_2 gas assisted conversion	ITO/NiO/ $Cs_{.17}FA_{.83}Pb(Br_{.17}I_{.83})_3$./$C_{60}$/BCP/Ag *(Cs- containing Double cation)*	1.02	19.7	76.0	16.2	[5]
NiO	Spray[d]	EA-Hex (100 µL)	ITO/NiO/$(FAPbI_3)_{0.85}(MAPbBr_3)_{0.15}$/PCBM/ZnO/Ag (*Cs-containing Tripe cation*)	1.10	22.6	73.0	17.3	**This work**

Where, [a] acetonitrile + ethanol (95:5 v%), [b] ethanol + acetylacetone, [c] deionized water, [d] ethanol + DI water (80:20 v%).

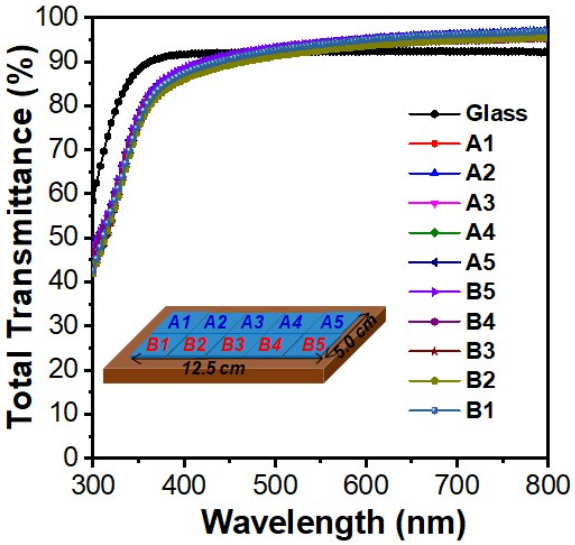

Fig. S5. Transmittance spectra of A1-A5 and B1-B5 samples deposited for 8 spray cycles

Table S3. Performance of perovskite devices fabricated on spray deposited large-area NiO-8 (62.5 cm^2) films (total 10 samples in two rows). The PSC devices are designated as 1 to 10.

Device	J_{sc} mA cm^{-2}	V_{oc} (V)	FF (%)	PCE (%)	R_s (Ω)	R_{sh} (Ω)
1	22.60	1.04	71.1	17.00	49.0	30515
2	21.94	1.06	70.96	16.66	50.3	23846
3	21.62	1.06	70.83	16.36	50.3	24606
4	21.81	1.06	70.97	16.51	49.3	23730
5	21.99	1.05	72.23	16.66	52.7	34080
6	22.92	1.06	70.27	17.23	49.9	26683
7	22.75	1.06	71.16	17.14	45.6	25493
8	22.56	1.06	71.58	17.06	45.6	26075
9	21.85	1.05	72.07	16.57	55.2	33276

10	21.78	1.05	71.80	16.49	56.2	26145

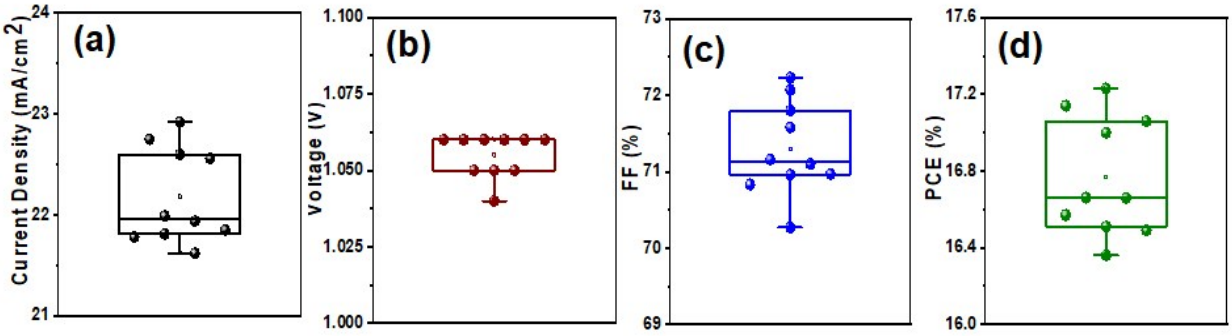

Fig. S6. Box plot of device parameters for samples A1-A5 and B1-B5.

Table S4. Performance of perovskite solar cells with variations in the active areas of the device.

Aperture Area (cm^2)	J_{sc} (mA cm^{-2})	V_{oc} (V)	FF (%)	PCE (%)	R_s (Ω cm^2)	R_{sh} (Ω cm^2)
0.07	22.75	1.06	71.16	17.14	3.2	1284.5
0.09	22.56	1.05	71.58	16.96	3.3	1780.4
0.52	22.76	1.07	56.90	13.93	11.32	751.7
1.04	22.51	1.06	51.23	12.22	14.56	443.1

Table S5. Summary of the synthesis method of the NiO*x* based (pristine and doped) HTL, PSC device structure, performance and device stability under different conditions for the inverted PSCs.

HTL	Synthesis method	Device structure	V_{OC} (V)	J_{SC} (mA/cm^2)	FF	PCE (%)	Stability	Stored environment	Ref.
Cu:NiO_x	Sol-gel	ITO/Cu:NiO_x/$MAPbI_3$/$PC_{61}BM$/bis-C_{60}/Ag	1.11	19.01	0.73	15.40	90% for 240 h	air	6
Cu:NiO_x	NP ink	ITO/Cu:NiO_x/$MAPbI_3$/C_{60}/BCP/Ag	1.12	22.28	0.81	20.26	95% for 1000 h	50–65% humidity	7
Cu:NiO_x	DCMS	FTO/Cu:NiO_x/$MAPbI_3$/PCBM/Ag	1.06	20.79	0.67	14.88	>90% for 10 days	30 °C, 60% humidity	8
NiO	DCMS	FTO/NiO_x/$MAPbI_3$/PCBM/Ag	0.99	18.76	0.57	10.54	>90% for 10 days	30 °C, 60% humidity	8
Cu:NiO_x	Sol-gel	FTO/bl-Cu:NiO_x/mpCu:NiO_x/$MAPbI_3$/ PCBM /bis-C_{60}/Ag	1.11	21.58	0.82	19.62	>90% for 1000 h	light	9
NiO	Sol-gel	FTO/bl-NiO_x/$MAPbI_3$/PCBM/bis-C_{60}/Ag	1.10	18.49	0.77	15.60	>90% for 1000 h	>90% for 1000 h	10
Ag:NiO_x	Sol-gel	ITO/Ag:NiO_x/$MAPbI_3$/$PC_{71}BM$/BCP/Ag	1.08	19.70	0.80	16.86	60% for 30 days	~30% humidity	10
NiO_x	Sol-gel	ITO/NiO*x*/$MAPbI_3$/$PC_{71}BM$/BCP/Ag	1.05	17.52	0.72	13.24	60% for 30 days	~30% humidity	10
Co:NiO_x	MS	FTO/Co:NiO_x/$MAPbI_3$/PCBM/Ag	1.01	20.02	0.63	12.63	>90% for 10 days	30 °C, 60% humidity	11
NiO_x	MS	FTO/NiO_x/$MAPbI_3$/PCBM/Ag	1.01	18.80	0.55	9.60	>90% for 10 days	30 °C, 60% humidity	11
Zn:NiO_x	Sol-gel	FTO/Zn:NiO_x/$MAPbI_3$/PCBM/BCP/Ag	1.10	22.80	0.78	19.6	84.4% for 30 days	Dry air	12
Li:NiO_x	Sol-gel	ITO/Li:NiO_x/$MAPbI_3$/PCBM/Ag	1.00	20.89	0.74	15.41	84.4% for 480 h	Glove box	13
Li:NiO_x	Sol-gel	FTO/LiNiO/$MAPbI_{3-x}Cl_x$/PCBM/Ag	1.12	21.79	0.74	18.00	~100% for 2 h	1 sun illumination	14
NiMgO	MS	FTO/NiMgO/$MAPbI_3$/PCBM/ZnMgO/Al	1.08	21.30	0.80	18.50	~90% for 600 h	50–70% humidity	15
Sr:NiO_x	Sol-gel	FTO/Sr:NiO_x/$MAPbI_3$/PCBM/AgAl	1.11	22.73	0.79	20.05	>60% for 100 days	18% humidity	16
NiO	Sol-gel	FTO/Sr:NiO_x/$MAPbI_3$/PCBM/AgAl	1.05	20.99	0.69	15.22	~32% for 100 days	18% humidity	16
Cs:NiO_x	Sol-gel	FTO/Cs:NiO_x/$MAPbI_3$/PCBM/ZrAcac/Ag	1.12	21.77	0.79	19.35	~90% for 80 days	Argon glovebox	17
Li, Ag:NiO_x	Sol-gel	ITO/Li, Ag:NiO_x/$MAPbI_3$/PCBM/BCP/Ag	1.13	21.29	0.80	19.24	95% for 30 days	30 ± 2% humidity	18
NiO	Sol-gel	ITO/NiO_x/$MAPbI_3$/PCBM/BCP/Ag	1.08	19.20	0.78	16.19	85% for 30 days	30 ± 2% humidity	18
La:NiO_x	Sol-gel	FTO/La:NiO_x/$MAPbI_3$/PCBM/BCP/Ag	1.01	21.02	0.73	15.46	95% for 30 days	Moisture-free	19
NiO_x	ALD	FTO/ALDNiO_x/$Cs_{0.05}MA_{0.95}PbI_3$/PCBM/ BCP/ALD-AZO/Ag	1.02	20.53	0.73	16.27	95% after 500 h	20-60% humidity, 1 sun	20
E-NiOx	NP ink	ITO/NiO_x/$MAPbI_3$/PCBM/ Ti(Nb)O_x /Ag	1.07	21.88	0.79	18.49	90% after 500 h	85 °C, 85% RH	21
NiOx	NP ink	FTO/NiO_x/$MAPbI_3$/PCBM/Ag	1.09	18.07	0.69	14.42	80% after 150 h	45-56 RH%	22
Li, Mg;NiO_x	Spray	FTO/NiMgLiO/$MAPbI_3$/PCBM/TiNbO/Ag	1.08	20.41	0.83	18.30	>90% for 1000 h	1 Sun light soaking	1
Li, Mg; NiO_x	Spray	FTO/NiMgLiO/$Cs_{0.05}FA_{0.15}MA_{0.8}PbI_3$/PCBM/BCP/Ag	1.08	22.55	0.79	19.17	~100% for 30 days	Dark, 55% humidity	23
Li, Mg; NiO_x	Spray	FTO/NiMgLiO/$MAPbI_3$/PCBM/BCP/Ag	1.08	21.75	0.75	17.60	30% for 15 days	Dark, 55% humidity	23
Li, Mg; NiO_x	Spray	FTO/ NiMgLiO/$MAPbI_3$/Ti(Nb)O_x/Ag	1.19	22.78	0.77	19.19	80% after 500 h	<25% humidity, 85°C	24
Li, Mg; NiO_x	Spray	FTO/ NiMgLiO/$FA_{0.85}MA_{0.15}Pb(I_{0.85}Br_{0.85})_3$ /Ti(Nb)O_x/Ag	1.08	21.98	0.79	18.75	90% after 1000 h	1 sun light soaking	25
Li, Mg; NiO_x	Spray	FTO/NiO_x/$FAPbI_3$/PCBM/TiO_x/Ag	1.10	23.09	0.81	20.65	80% after 500h	85 °C	26
NiO	Spray	ITO/NiO/$Cs_{17}FA_{83}Pb(Br_{17}I_{83})_3$ /C_{60}/BCP/Ag	1.02	19.7	0.76	16.2	~90% after 4000 h	N_2 atmosphere	5
NiO	Spray	ITO/NiO/$Cs_4(MA_{0.17}FA_{0.83})_{96}Pb(I_{0.83}Br_{0.17})_3$/PCBM/ZnO/Ag ITO/NiO/$Cs_4(MA_{0.17}FA_{0.83})_{96}Pb(I_{0.83}Br_{0.17})_3$/PCBM/ZnO/Au	1.06 1.06	22.9 22.9	0.72 0.72	17.3 17.3	>87% after 4500 h >82% after 200 h	N_2 atmosphere 85 °C; 85% RH	**This work**

Note- DCMS- DC magnetron sputtering, ALD- Atomic layer deposition, MS- magnetron sputtering.

References:

1. W**.** Chen, Y. Wu, Y. Yue, J. Liu, W. Zhang, X. Yang, H. Chen, E. Bi, I. Ashraful, M. Gratzel, L. Han, *Science,* 2015, **350**, 944-948.
2. M. Yin, F. Xie, H. Chen, X. Yang, F. Ye, E. Bi, Y. Wu, M. Cai and L. Han, *J. Mater. Chem. A*, 2016, **4**, 8548-8553.
3. W. Chen, Y. Wu, J. Liu, Ch. Qin, X. Yang, A. Islam, Y.-B. Cheng, L. Han, *Energy Environ. Sci.*, 2015, **8,** 629-640.
4. Y. Qin, J. Song, Q. Qiu, Y. Liu, Y. Zhao, L. Zhu, Y Qiang, *J. Alloys. Compd.,* 2019, **810,** 151970.
5. W. J. Scheideler, N. Rolston, O. Zhao, J. Zhang, R. H. Dauskardt, *Adv. Energy Mater.,* 2019, **9,**1803600.
6. J. H. Kim, P. W. Liang, S. T. Williams, N. Cho, C.C. Chueh, M. S. Glaz, D. S. Ginger, A. K. Y. Jen, *Adv. Mater*., 2015, **27,** 695–701.
7. W. Chen, Y.H. Wu, J. Fan, A.B. Djurisic, F.Z. Liu, H.W. Tam, A. Ng, C. Surya, W. K. Chan, D. Wang, Z. B. He, *Adv. Energy Mater.,* 2018, **8,** 1703519.
8. A. B. Huang, L. Lei, Y. X. Chen, Y. Yu, Y. J. Zhou, Y. Liu, S.W. Yang, S. H. Bao, R. Li, P. Jin, *Sol. Energy Mater. Sol. Cells*, 2018, **182**,128–135.
9. K. Yao, F. Li, Q.Q. He, X.F. Wang, Y.H. Jiang, H.T. Huang, A.K.Y. Jen, *Nano Energy,* 2017, **40**, 155–162.
10. Y. Wei, K. Yao, X.F. Wang, Y.H. Jiang, X.Y. Liu, N.G. Zhou, F. Li, *Appl. Surf. Sci*., 2018, **427,** 782–790.
11. A. B. Huang, J. T. Zhu, J. Y. Zheng, Y. Yu, Y. Liu, S. W. Yang, S. H. Bao, L. Lei, P. Jin, *J. Mater. Chem. C*, 2016, **4,** 10839–10846.

12. Y. J. X. Wan, Z. Qiu, H. Zhang, X. Zhu, I. Sikandar, X. Liu, X. Chen, B. Cao, *ACS Appl. Energy Mater*., 2018, **1**, 3947–3954.

13. M. A. Park, I.J. Park, S. Park, J. Kim, W. Jo, H. J. Son, J. Y. Kim, *Curr. Appl. Phys*., 2018, **18,** S55–S59.

14. W. Y. Nie, H. H. Tsai, J. C. Blancon, F. Z. Liu, C. C. Stoumpos, B. Traore, M. Kepenekian, O. Durand, C. Katan, S. Tretiak, J. Crochet, P. M. Ajayan, M. G. Kanatzidis, J. Even, A. D. Mohite, *Adv. Mater*., 2018, **30**, 170387.

15. G. J. Li, Y. B. Jiang, S. B. Deng, A. W. Tam, P. Xu, M. Wong, H. S. Kwok, *Adv. Sci.*, 2017, **4**,1700463.

16. J. K. Zhang, W. J. Mao, X. Hou, J. J. Duan, J. P. Zhou, S. M. Huang, O. Y. Wei, X. H. Zhan, Z. Sun, X. H. Chen, *Sol. Energy*, 2018, **174**, 1133–1141.

17. W. Chen, F. Z. Liu, X. Y. Feng, A. B. Djurisic, W. K. Chan, Z. B. He, *Adv. Energy Mater.,* 2017, **7**, 1700722.

18. X. Xia, Y. Jiang, Q. Wan, X. Wang, L. Wang, F. Li, *ACS Appl. Mater. Interfaces*, 2018 **10 (51)**, 44501–44510.

19. S. Teo, Z. L. Guo, Z. Xu, C. Zhang, Y. Kamata, S. Hayase, T. Ma, *Chem. Sus. Chem.*, 2018, **12 (2)**, 518–526.

20. S. Seo, S. Jeong, C. Bae, N. G. Park, H. Shin, *Adv. Mater.*, **30,** 2018, 1801010.

21. J. He, E. Bi, W. Tang, Y. Wang, Z. Zhou, X. Yang, H. Chen, L. Han, *Sol. RRL*, 2018,**2**, 1800004.

22. G. D. Niu, S. Y. Wang, J. W. Li, W. Z. Li, L. D. Wang, *J. Mater. Chem. A*, 2018, **6,** 4721–4728.

23. X. Yin, M. Que, Y. Xing and W. Que, *J. Mater. Chem. A*, 2015, **3**, 24495–24503.

24. Y. Wu, F. Xie, H. Chen, X. Yang, H. Su, M. Cai, Z. Zhou, T. Noda, L. Han, *Adv. Mater.,* 2017, **29**, 1701073.

25. Y. Wu, X. Yang, W. Chen, Y. Yue, M. Cai, F. Xie, E. Bi , A. Islam, L. Han, *Nat. Energy,* 2016, **1,** 16148.

26. F. Xie, C.C. Chen, Y. Wu, X. Li, M. Cai, X. Liu, X. Yang, L. Han, *Energy Environ. Sci.,* 2017, **10**, 1942.